BNL-105815-2014-TECH

EP&S No. 100;BNL-105815-2014-IR

20 Kilogauss solenoid magnet

J. Li

August 1981

Collider Accelerator Department

Brookhaven National Laboratory

U.S. Department of Energy

USDOE Office of Science (SC)

DISCLAIMER

Accelerator Department

BROOKHAVEN NATIONAL LABORATORY
Associated Universities, Inc.

EP&S DIVISION TECHNICAL NOTE

NO. 100

20 KILOGAUSS SOLENOID MAGNET

Jia Li*, G.Y. Fang*
Massachusetts Institute of Technology
Laboratory for Nuclear Science

J.C. Walker
Brookhaven National Laboratory

*Home address: Institute of High Energy Physics, Peking, China

20 Kilogauss Solenoid Magnet

Jia Li*, G.Y. Fang*
Massachusetts Institute of Technology
Laboratory for Nuclear Science

J.C. Walker
Brookhaven National Laboratory

ISA experiments with good mass resolution require an accurate drift chamber with long internal signal wires in a high axial magnetic field. This report describes an inexpensive magnet designed and fabricated to test a full-length model of such a chamber having, however, 9 wires only. The magnet generates a solenoidal field with a coil of 12.5" diameter and 16.8" length. Slots in the structure allow a beam to pass through the center orthogonal to B.

The magnet is a 20 kilogauss solenoid magnet with a field uniformity $\leq$ 1% over the fiducial volume of the chamber (16 x 10 cm).

*Home address: Institute of High Energy Physics
Peking, China

INTRODUCTION

Study of narrow structures and heavy resonances at ISABELLE energies will require good mass resolution, hence extremely accurate drift chambers recording the tracks in high magnetic fields[1] B, of 15 kgauss. Since the resolution increases as $B\ell^2$, the radial distance ℓ must be ~2 meters to reach 1% mass resolution. To have a substantial (>70%) solid angle, this implies 5 m long wires. Since 5 m long wires in fields as high as 15-20 kgauss and at 4 atm gas pressure have not been operated, a full-length module of 9 wires was developed (Figure 1) which resembles the outer 9 wires of a full-size detector chamber at ISABELLE (worst case). The wire and mechanical alignments were done in the way envisioned for the full chamber. However, the pressure vessel is reduced to an 11" diameter aluminum tube supported on a very solid structure (Figure 2a). To minimize multiple scattering, windows of mylar foil 10 mils thick let the beam pass. At the point of measurement the solenoid generates a field $\geq$15kG as in the full chamber, which deflects the drifting electrons by a substantial angle. This, together with gravitational sag, electrostatic forces, and mechanical vibrations, will influence the final accuracy to be obtained. To achieve a wire accuracy of 140 µm and a mass resolution of 1%, the magnetic field must be homogeneous to < 1% if we are to avoid the necessity of introducing other corrections.

Figure 2b gives the cross section in the beam for the magnet fulfilling this requirement over the fiducial volume as indicated by the chamber cross section. Magnet, pressure tube, and chamber were mounted on a strong back with a mechanism moving it up and down through the test beam A2 (see Figure 3).

DESIGN CONSIDERATIONS

The test system requires a field uniformity of better than 1% in the chamber regions and a field strength of 1.5 T. The available power supply has maximum current of 3600 A. Having these parameters together with the inner diameter, we first chose the lengh of the magnet. This was done by optimizing the field strength and uniformity against the coil length while keeping other parameters fixed. With 12.5" inner diameter, a length of 17" is sufficient in the sense that the central field is not rapidly increasing as the length and the field homogeneity in the central chamber region is better than 1%.

According to Ampere's Law, for an infinitely long solenoid:

$$\int \vec{B} \cdot d\vec{l} = N \mu_o I.$$

We have

$$B = \mu_o n \cdot I$$

where $n \cdot I$ is the Ampere turns per unit length. For B = 20 kgauss we have

$$n \cdot I = \frac{2.0\ T}{4\pi \cdot 10^{-7}\ N/A^2} = 1.59 \cdot 10^6\ \frac{A\text{-turns}}{m}$$

For our finite length solenoid we will need approximately 18% more A • turns, as we will see later. Reaching 20 kgauss with 3600 A requires the coil to have

$$N = \frac{1.59 \cdot 10^6\ A \cdot turns \cdot 0.43\ m}{3600\ A\ m} \cdot 1.18 = 224\ turns$$

The available voltage of max 150 V allows a resistance of 0.042Ω, hence the copper conductor was chosen to be 1/2" x 1/2" with a central hole of 1/4" diameter for

water passage. The dissipation of 550 KW requires water flow of 50 gallons/minute at a ΔT of about 50^{o} C. The thickness of the iron return yoke and end cap was determined in such a way that minimum iron was used to obtain desired field and field uniformity. Spacer thickness was optimized to get best field uniformity. Final analysis was done on the BNL computer using a program called "Poisson" which was developed at L.B.L. The main parameters of the magnet thus chosen are listed in Table 1.

Table 1

Main Parameters of the Magnet

central field	20 kG
total amp turns	$8.1 \cdot 10^5$ A
operating current	3600 A
operation voltage (total)	150 V
field uniformity	< 1%
total turns	224
inductance	0.01 H
power consumption	544 KW
inner diameter	12.5"
effective length	16.8"
gap width (max)	1.8"
window size	0.7" x 8"
conductor weight	~900 lb
total weight	~7100 lb
water consumption	38 gal/min
water pressure drop at the manifold	207 psi
water temperature rise	110° F
water temperature limit	190° F

MANUFACTURING

The core

The core (see Figures 4 and 5) was made out of low carbon steel laminates and assembled with bolts. All parts, where possible, were flame cut from existing stock. Central hole, conductor paths, window openings, lifting lugs, etc., were formed by flame cutting from properly selected laminates. Machining was kept to a minimum. The core was made as symmetrical as possible within the limitation of manufacturing cost considerations in order to achieve best field uniformity. The central hole in each of the 6 inch thick ends is only 1/2 inch larger than the coil bore. The "window" (an opening completely through the core to allow passage of protons between the coils and through the drift chamber) is approximately 0.7 inches wide by 8 inches high, and pierces approximately $4\frac{1}{2}$ inches of iron on each side.

The coils

The two coils (see Figures 8, 9) were to be wound identically except for the orientations of water fittings in order to achieve better field uniformity. The ends facing each other are kept parallel in the best possible way. The nonconductor, or air wedge, is an unavoidable end condition of every large conductor coil which is layered and wound helically. The volume of the wedge was minimized by winding successive layers in opposite directions, as can be seen from Figure 8 and Figure 9. Their effects on magnetic field uniformity can be further reduced by assembling the coils in such a way that the conductor faces the air wedge across the coil gap.

Each of the two coils consists of 8 layers of 14 turns. Unlike a normal solenoid with two leads, these coils have 8 leads in and 8 leads out. Non-uniformity induced by the multiple end leads is minimized in the gap by current flowing in opposite directions in adjacent leads. The total amount of conductor used for the two coils is about 900 pounds.

The coils were wound on a simple and convenient winding machine designed in-house. The machine consists of a low speed, high torque turntable and a vertical spindle serving as the holder of the forms on which the coils were wound. The turntable, being able to rotate both forward and backward, can be excellently controlled. Winding tension is maintained by passing the conductor through Teflon-lined clamps attached to a secured, height-adjustable table which can be adjusted vertically to keep approximately level among the conductor roll, clamps, and the layer of the magnet being wound. A tool to wrap the fiberglass tape (0.007 inch thick) onto the conductor for insulation mechanically during the winding process was incorporated in the line, saving a great deal of time needed to wrap the insulation tape manually. A sketch of the machine is shown in Figure 6. Figure 7 is a picture of the winding process.

Both coils were wound on the same strong alumininum cylinder. Removal of the coils from the form was made possible by inserting two layers of Teflon and one layer of metal sheet between cylinder and windings. An end plate was attached to the cylinder for applying pressure axially and restraining the leads. After completion of each layer, pressure was imposed axially and diametrically through the end plate and hose clamp to tighten up the windings. Then the coil was immersed in epoxy to fill all the voids in the winding so that the conductor forms a solid block and keeps designed shape. Before winding of the next layer the coil was smoothed to prevent tearing or dislodging the tape on the conductor to be wound. This process was repeated eight times per coil. The leads were bent with smallest possible radius, and kept tight against each other. Finally, each coil was

covered with a layer of fiberglass tape and was epoxy-impregnated and cured. Each layer was wound opposite to the preceding one for field uniformity as discussed.

Finally, both electric and hydraulic connections and water fittings were connected. Figure 10 is a picture of a finished coil.

In the assembly process neoprene and micarta shims were used to center the coils and to protect them from metal edges. Two pipe and flare fitting manifolds were added for inlet and outlet of the water supply. Rubber water hoses connect the manifolds to the proper coil interconnectors. Each rubber hose serves two coil layers so that 8 sets of hoses feed a total of 16 water paths in parallel. To insure against overheating, temperature sensing switches (KLIXON's) were attached to the return side of each layer. The power supply will be shut down automatically if any of the sensors detect a temperature higher than 190^{o}F. Finally, two terminal plates per coil (4 total) were added and clamped to appropriate coil leads in such a manner that the coil interconnectors plus one external jumper formed a series path through both coils.

Test procedure and the results

In the first test the magnet reached a current of only about 2700 A because of the lack of cooling power and improper triggering of the temperature sensor. After cutting the two manifolds into four, thus increasing the water flow by an appreciable amount of 7 gallons/min. and replacing the temperature sensors, the magnet reached a maximum current of 3600 A, which corresponds to a central field of about 20.1 kG. Figure 11 shows characteristic cooling curves of the magnet after modifications on the manifold. It can be seen that the extrapolated temperature rise ΔT corresponding to 3600 A at outer layers is about 60^{o}C which is 10^{o}C higher than the designed value. The magnet, running at 3600A, reached the temperature limit of the outer layers (190^{o}F) and was triggered off in a short time .

The magnet was designed to run only for 10 min. intervals at highest fields and therefore has no big cooling margin. Increasing the water flow, either by increasing the pressure of input or by pumping the output can give long time running at 20kG.

Magnetic field was measured by a precision temperature-compensated Hall probe, which was calibrated against a standard search coil to 10^{-3}. The Hall probe was attached to a ruler which slid on a holder so we could measure the field of various positions, as can be seen in Figure 12a. The probe has a sensitivity of 31.5 mV/kG. Using a voltmeter accurate to 0.1 mV, we measured with a relative accuracy of $2 \cdot 10^{-4}$ at 15 kG and an absolute accuracy of 3 gauss, which is satisfactory for our purpose. The results for our magnet are summed up in Figures 12-16. Field distributions along the radial direction on the middle plane and along the symmetry axis are plotted in Figure 12 and Figure 13 respectively, where the dotted line denotes the calculated value. Field variations along x direction for different y are plotted in Figure 14 for 2750A, with x, y defined in the figure. One notes a quite appreciable difference in field and field distribution as one goes from the center off along x direction and along y direction. This seems to be in contradiction with the fact that a solenoid has cylindrical symmetry, demanding B to be the same for constant distance to the center. This comes from the fact that the defined y direction is the direction of the current leads where the effective current density is lower than the rest of the coils. Therefore, deviations along y represent the worst case. We note also that there is a left-right asymmetry on all the field distribution curves shown in Figure 14. This comes from the unequal spacing (~0.8 cm) between the coil ends and the iron end caps of the left and right sides with respect to the y axis, caused by assembly errors.

Figure 15 gives the magnetic field B as a function of the current I whose non-linearities are a measure of the degree of saturation of the iron. If the iron is saturated, the field contribution from magnetization of the iron will decrease; therefore, the curve will bend toward right bottom. It can be seen that up to the highest current, there is no saturation visible in accordence to the design. As a matter of fact, saturating effects could be noticed in the field distribution of the magnet at different current levels. If the magnet cores were saturating it would show different field distributions in shape for different currents. Figure 16 gives the field variation in the middle plane at the highest currents. The identical shape of the curves confirms preceding observations. The field uniformity on the middle plane for the chamber region can be obtained from Figure 14.

$$B_e(x = \pm 5) - B(x = 0) = 1.510 - 1.506 = 0.26\%$$

where B_e and B_o stand for the field at the edge of the chamber on the middle plane and the field at the center respectively.

The deviation of measured field from computed value is about 1.4%, which is within the manufacturing accuracy and steel quality variation. At 3600 A, if the magnet were an infinite solenoid, the magnet field strength would be

$$B_o = \mu_o \frac{NI}{\ell}$$

$$= \frac{4\pi \cdot 10^{-7}\ N/A^2 \cdot 224 \cdot 3600 \cdot A}{0.43\ m}$$

$$= 23.6\ kG$$

while the measured value is only 20.1.

The deviation of 17.4% is mostly due to the opening at the end caps and the center.

The manufacturing of the magnet shows that a reasonably precise magnet does not have to be made in a very expensive way.

ACKNOWLEDGEMENTS

We would like to thank M.I.T. and Professor S.C.C. Ting for making our USA stay possible, and Professor U. Becker and Dr. G. Danby for their helpful direction. We are greatly appreciative of the hospitality tendered by Professor D. Lowenstein of the A.G.S. at BNL, and are particularly indebted for the technical and construction help of Harold (Swede) Knudsen and George Korhut.

References

1. Precision Drift Chamber Development Project, BNL T20, U. Becker et al.
2. "Electromagnetic Theory," Julius Adams Stratton, 1941

FIGURE CAPTIONS OF SECTION 10:

Figure 1 Cross section through 9-wire chamber

Figure 2 Sketch of the test system

Figure 3 Test beam arrangement at BNL

Figure 4 Schematic of the magnet

Figure 5 Core laminates

Figure 6 Coil winding schematic

Figure 7 A photo of winding process

Figure 8 Schematic end view

Figure 9 Schematic cross section

Figure 10 A photo of finished coils

Figure 11 Cooling characteristics of the magnet

Figure 12 Field along central radial line at 2750 A (measured and calculated) with a sketch of the measurement device

Figure 13 Field along z-axis at 2750 A (measured)

Figure 14 Field along x,y at 2750 A (measured) with x,y defined in the figure

Figure 15 The magnet excitation curve

Figure 16 Field along radial direction on the middle plane at highest currents (measured)

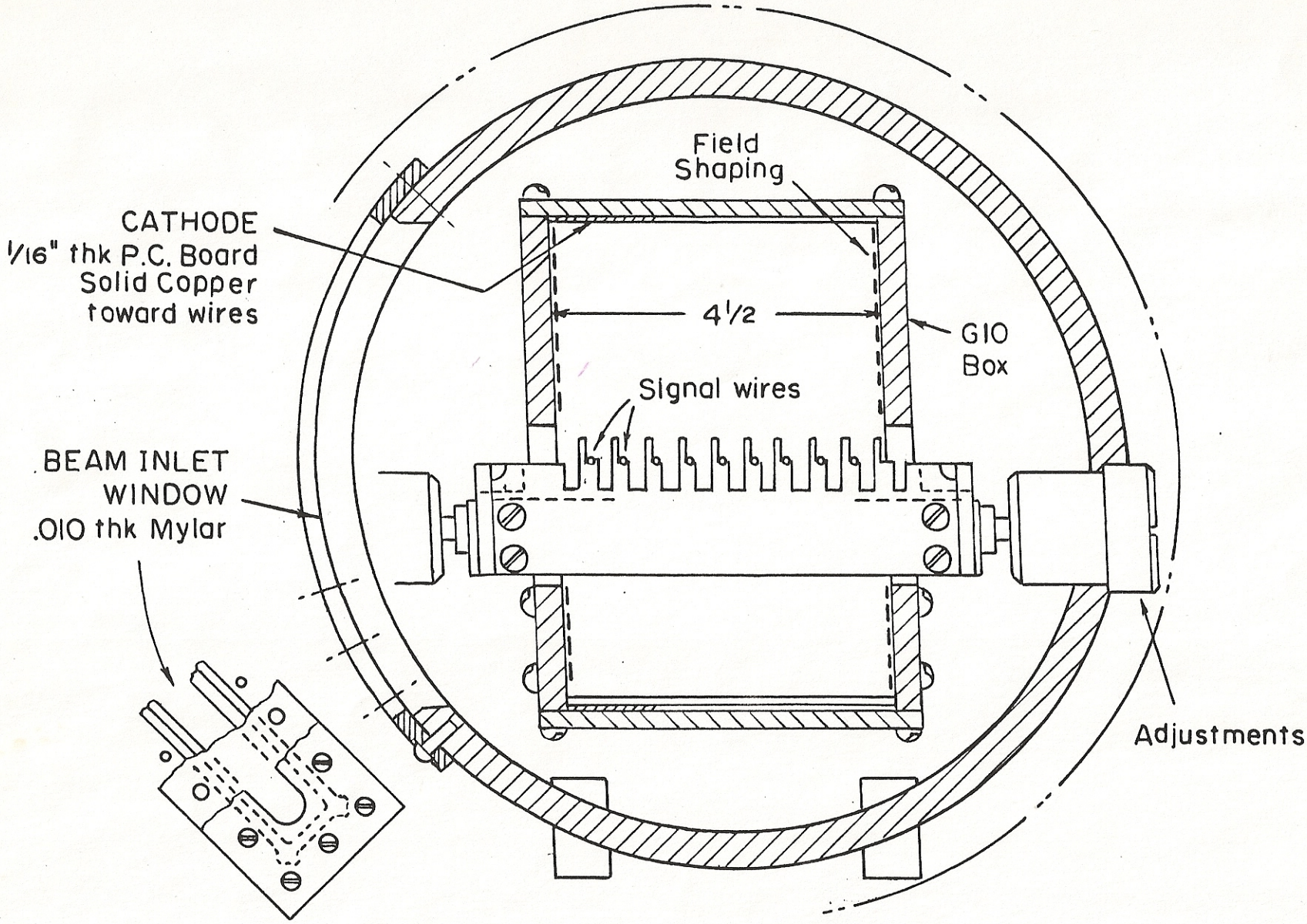

Fig. 1 Cross section through 9-wire chamber
One of three wire supports is shown

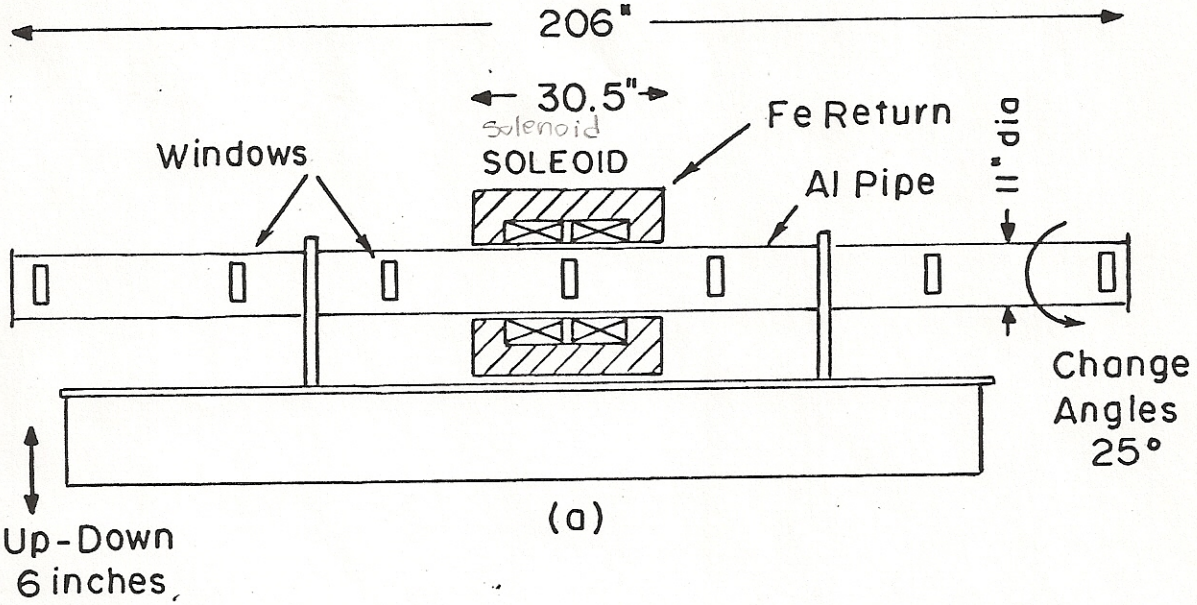

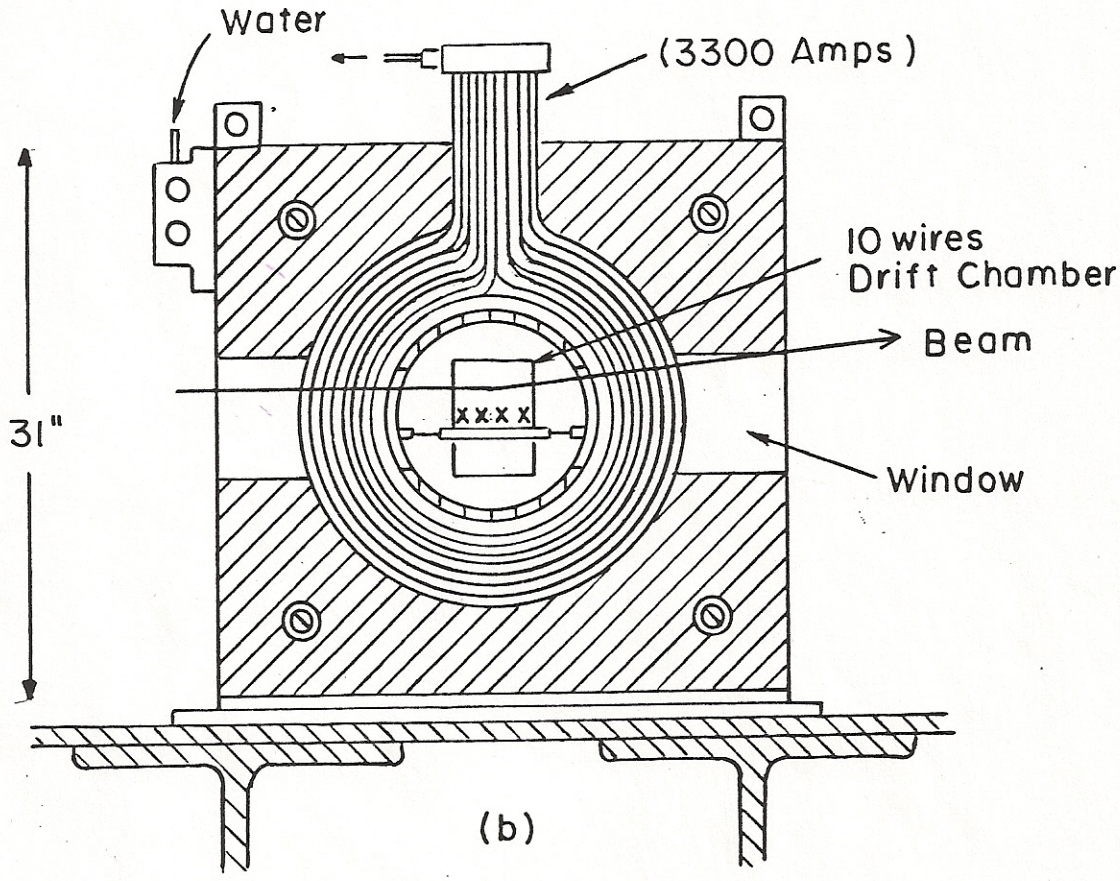

Fig. 2 (a) Sketch of the pressure type housing the 9-wire chamber and solenoid

(b) Cross section of the magnet at the beam line

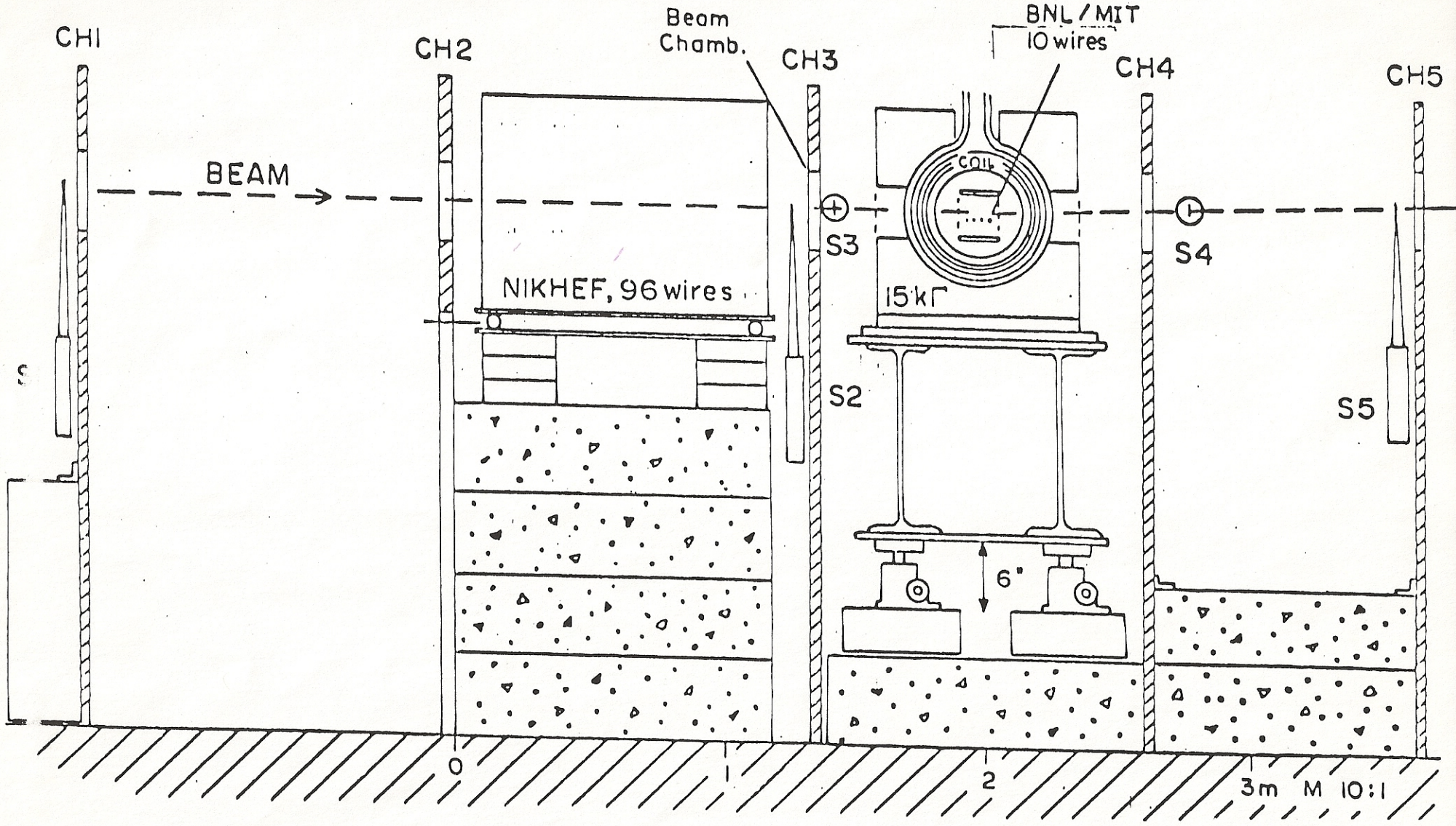

Fig. 3 Test beam arrangement at BNL A2 line

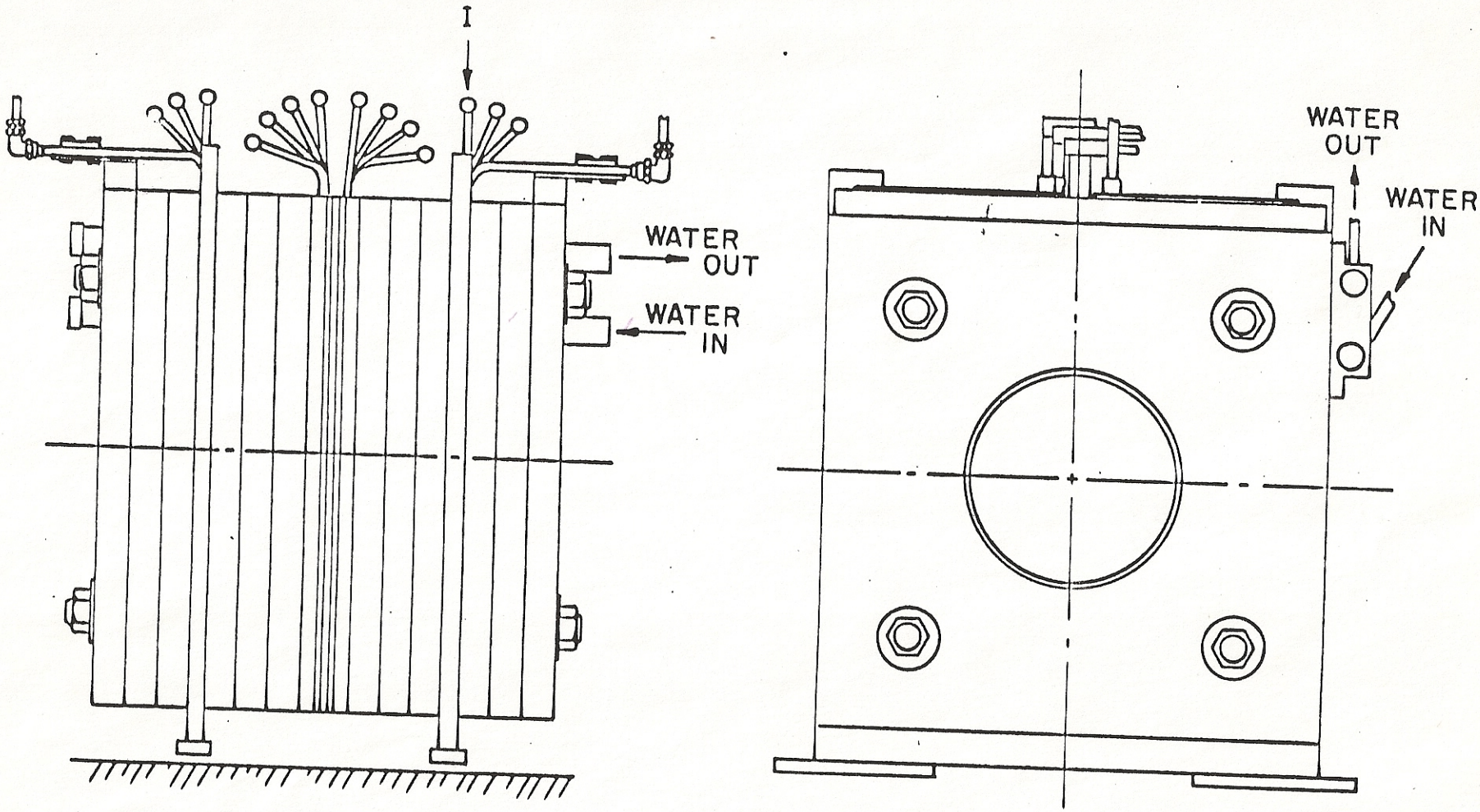

Fig. 4 Schematic of the magnet

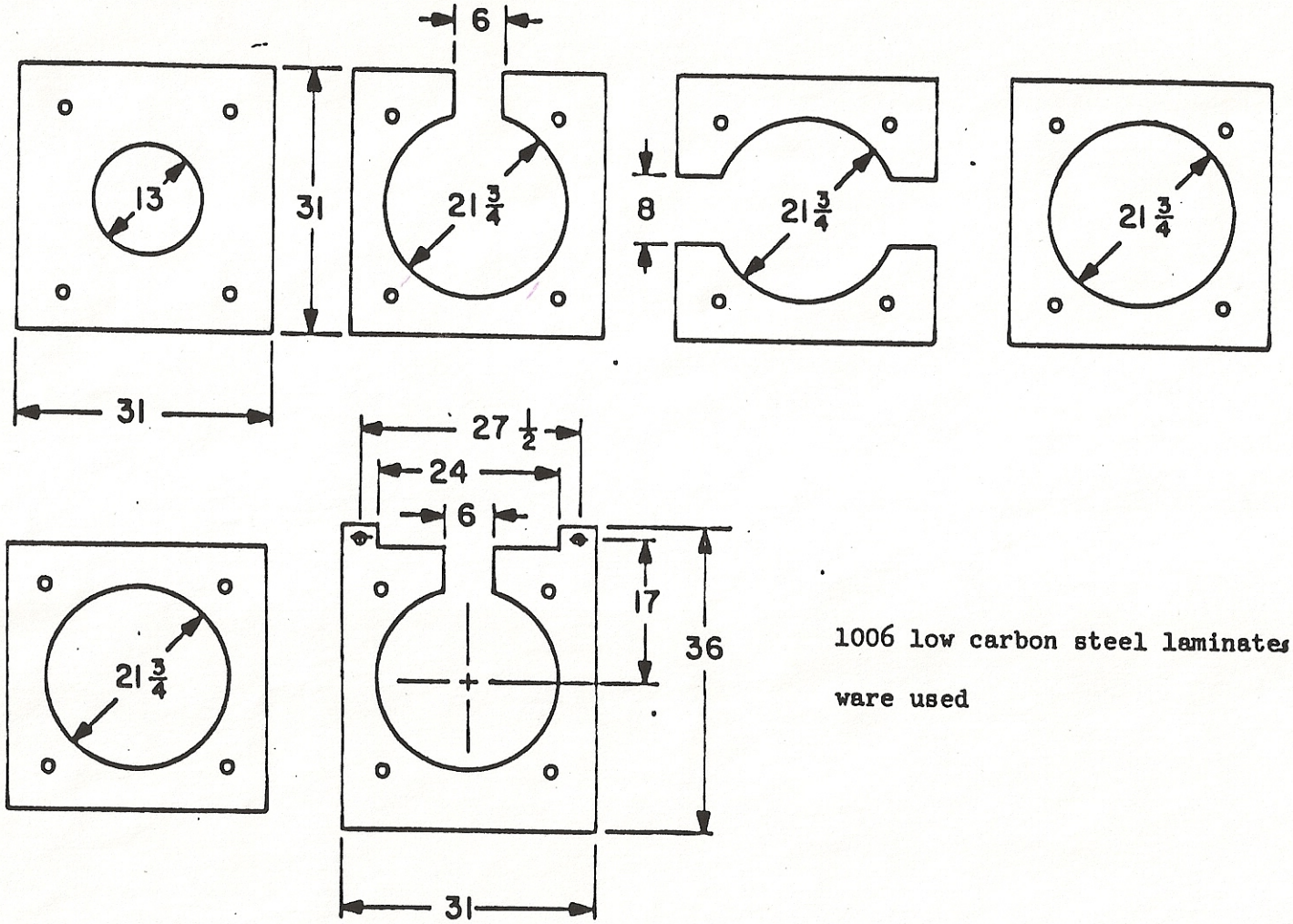

1006 low carbon steel laminates ware used

Fig. 5 Core laminates sketch

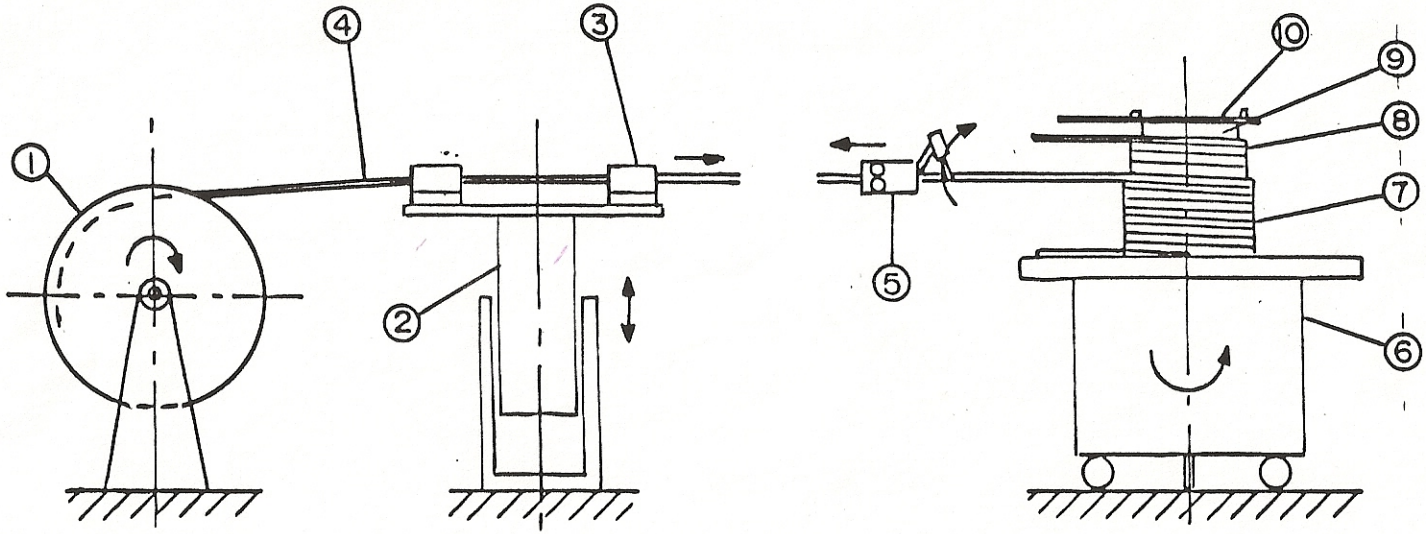

1 Copper Conductor Supply Roll
2 Adjustable Height Table
3 Teflon-lined Tension Clamps
4 Conductor
5 Tool for Fiberglass Tape-wrapping
6 Rotating Table
7 Coil being wound
8 Coil already wound
9 Coil Form
10 Lead Retainer/Coil Clamp

Fig 6 COIL WINDING SCHEMATIC

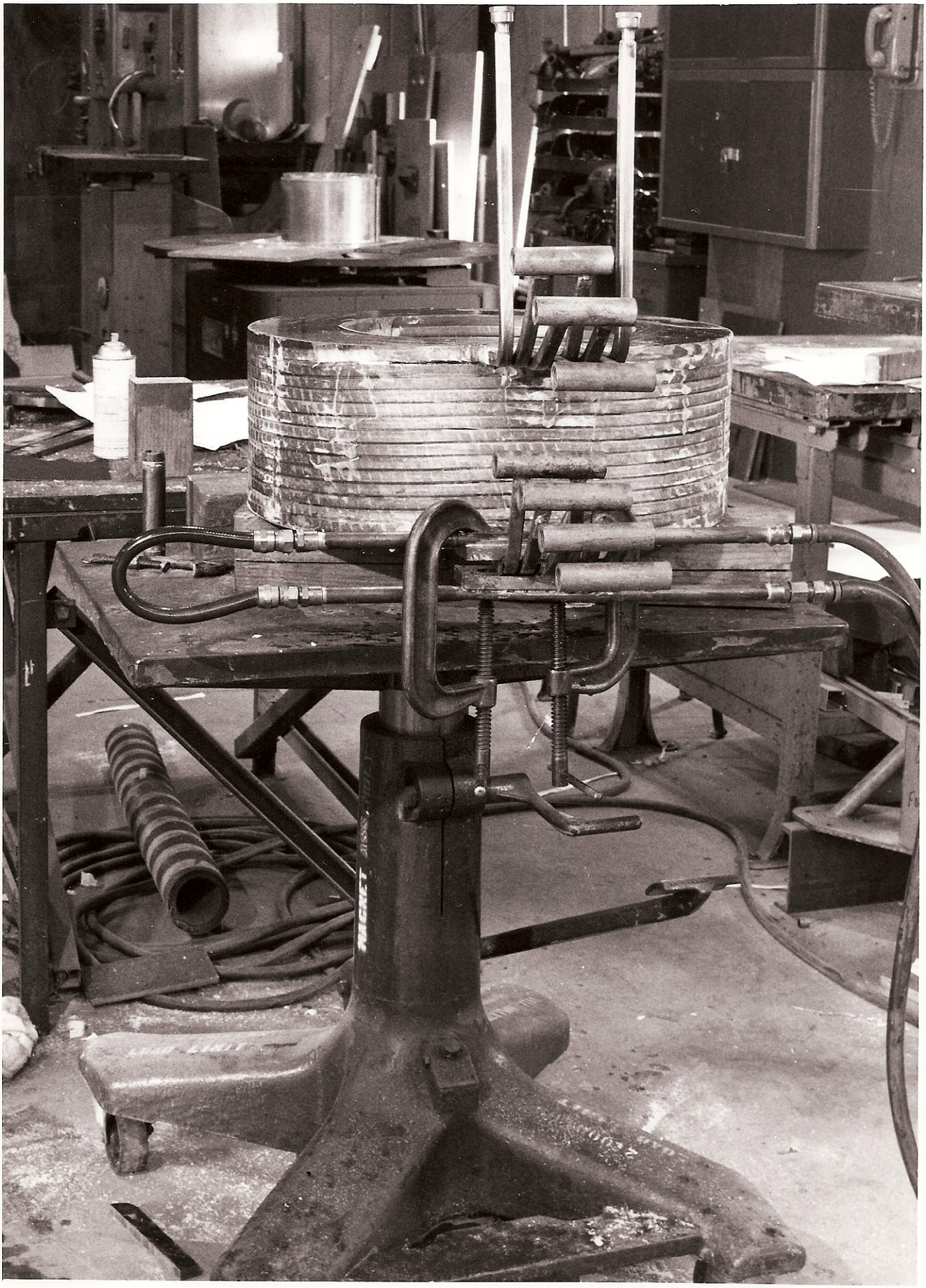

Fig. 7. Winding Process

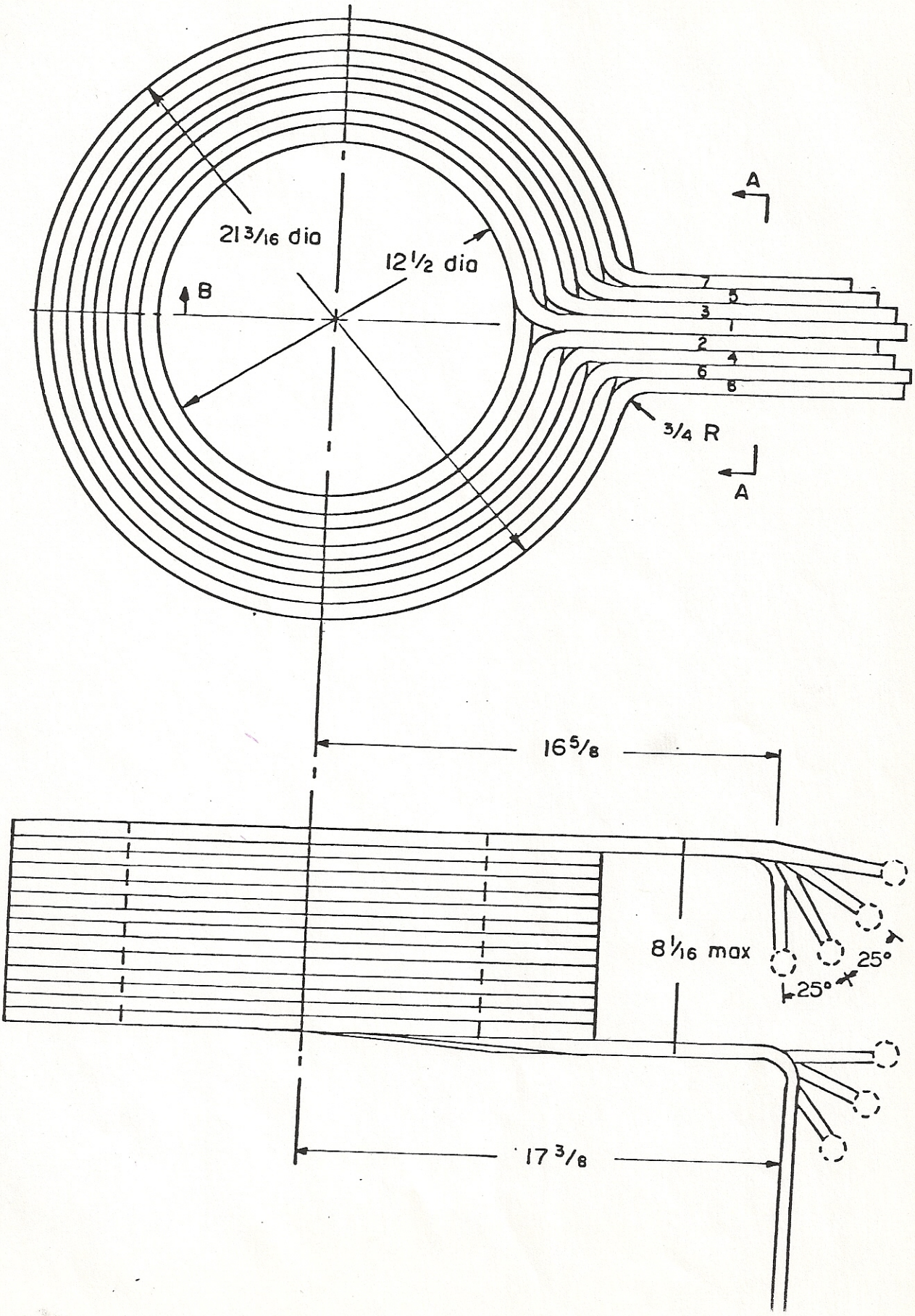

Fig 8. The Coil Schematic

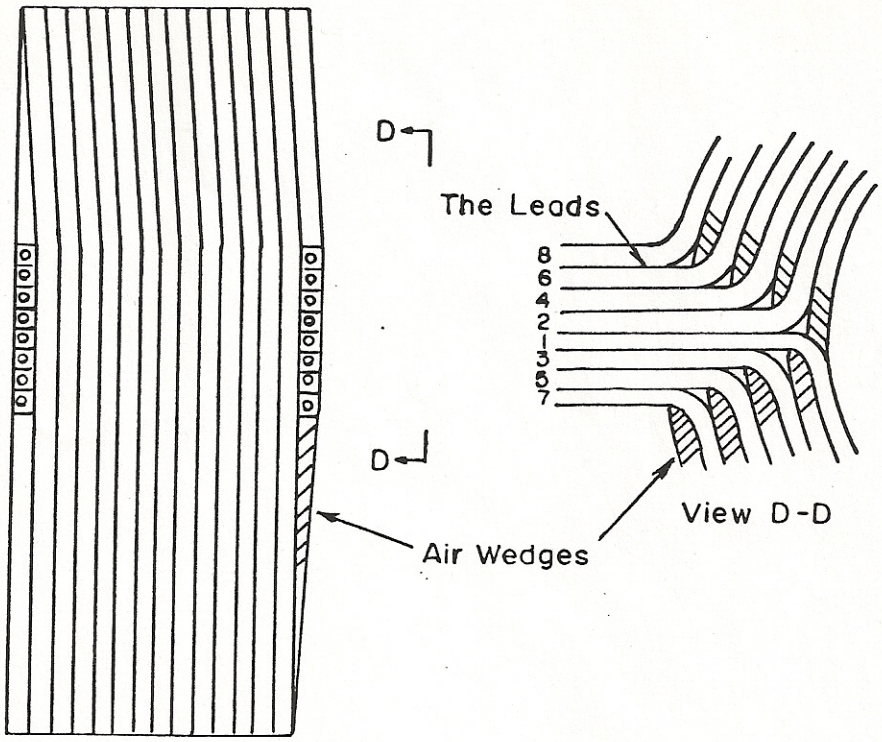

A-A Section

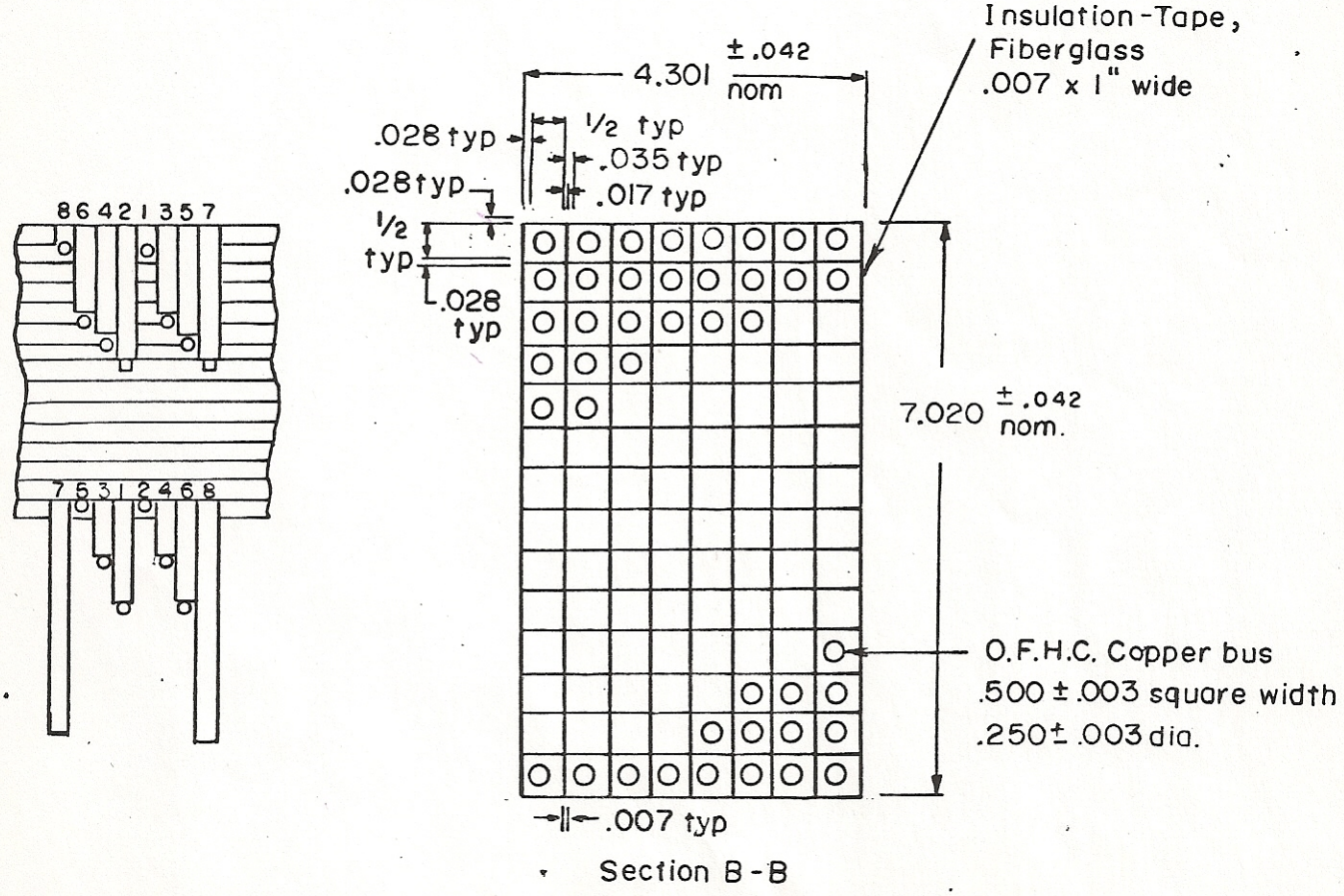

Section B-B

Fig. 9 Details of the Windings

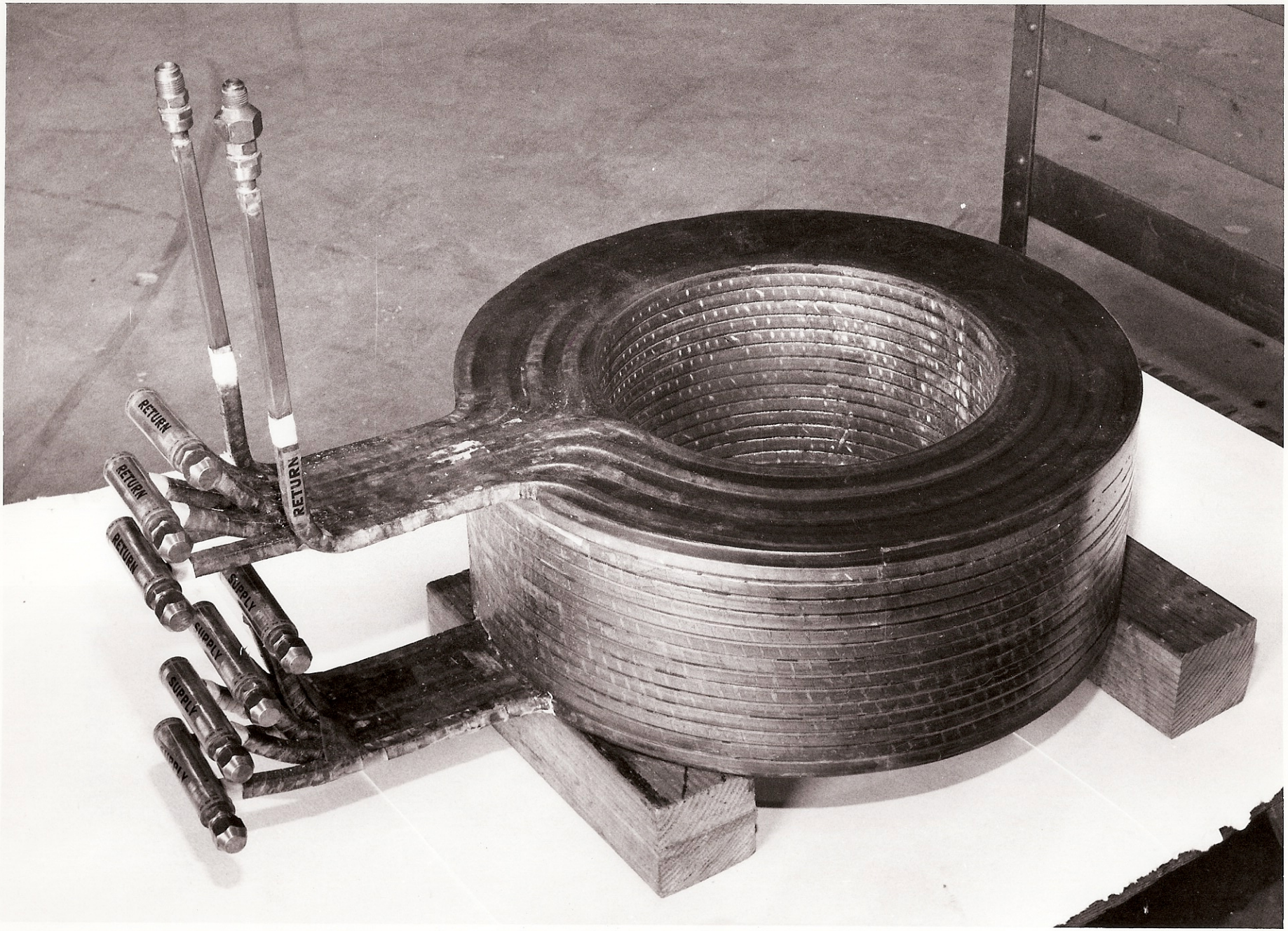

Fig. 10. Finished coil

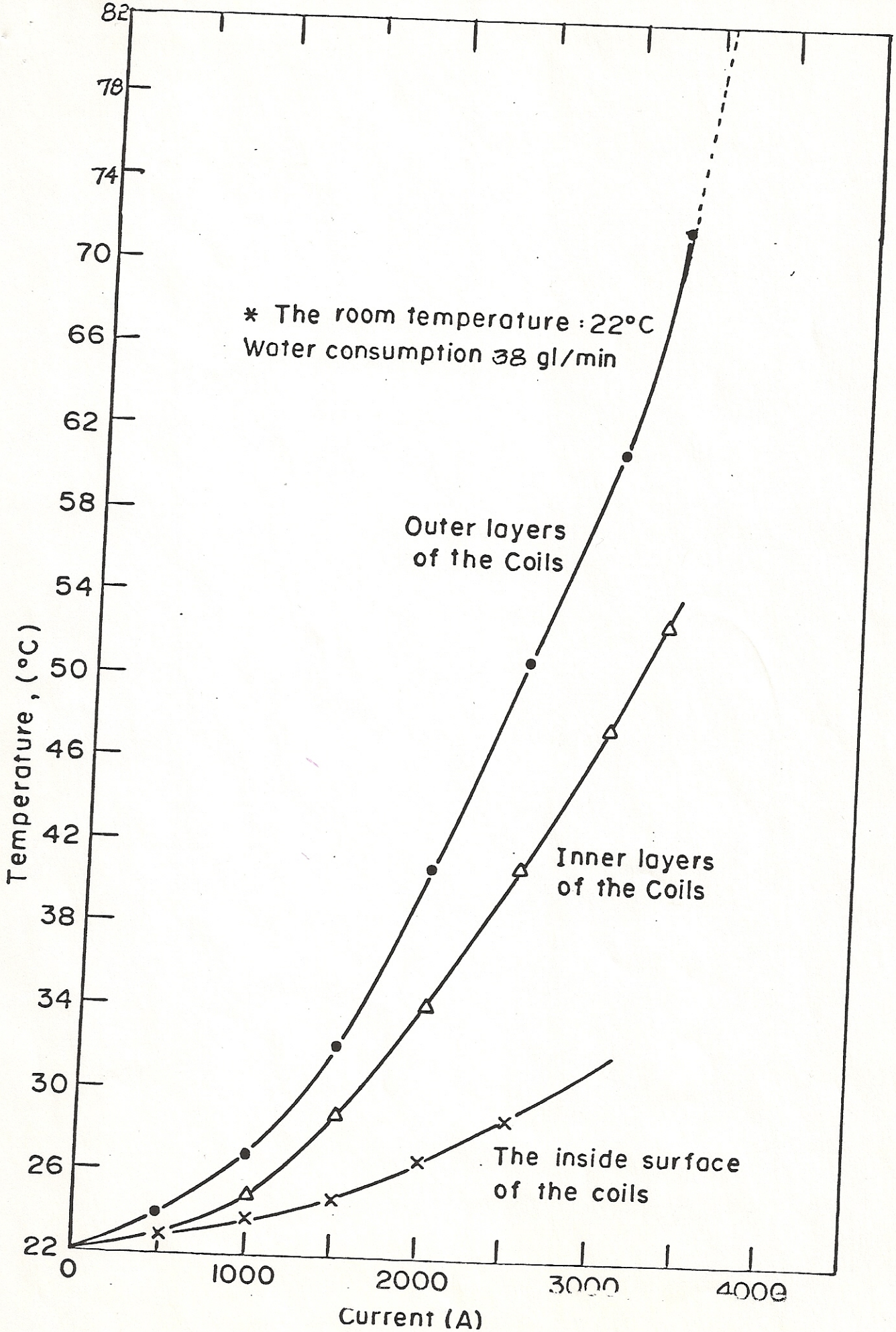

Fig. 11 Cooling Characteristics of the Magnet

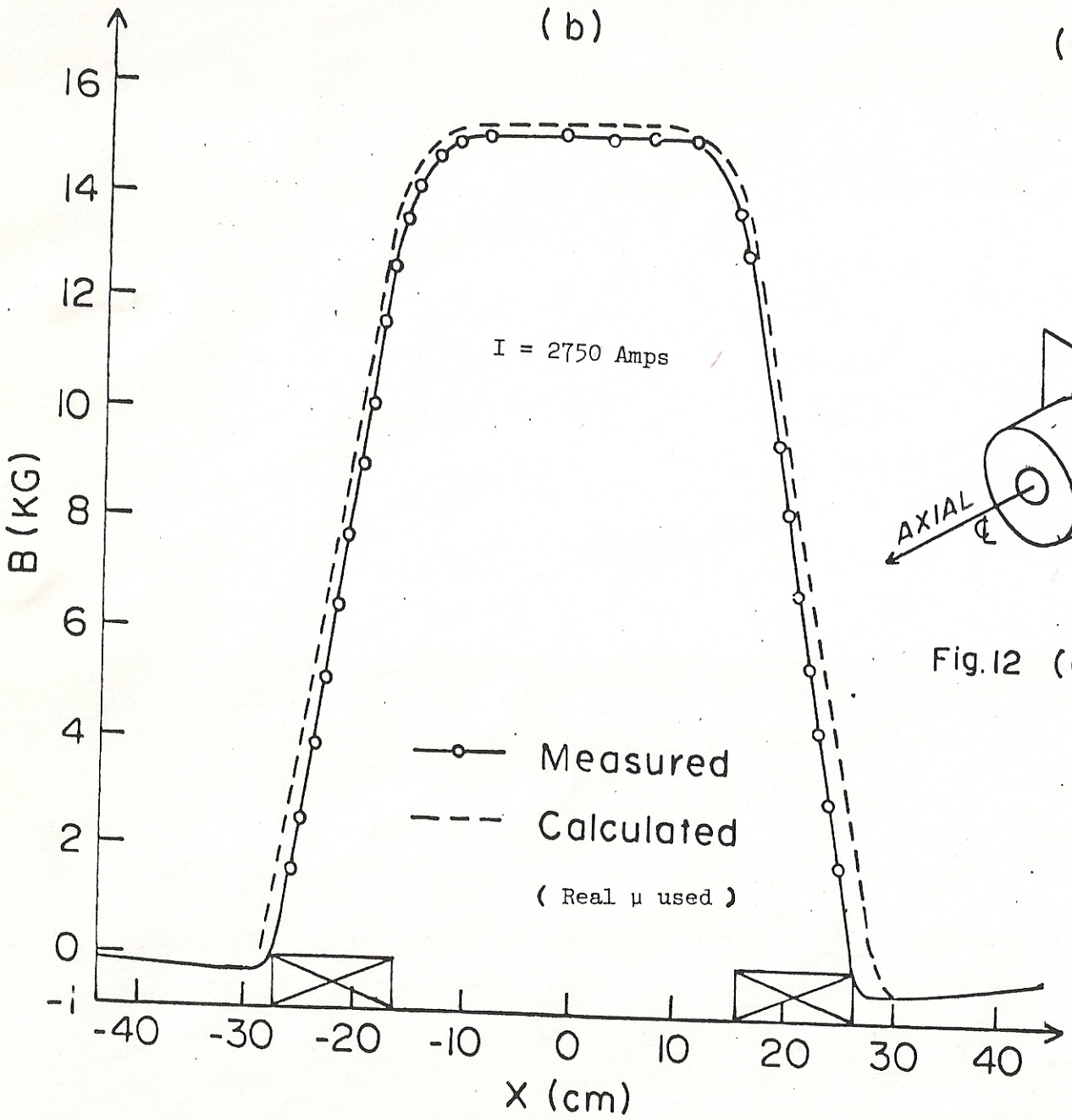

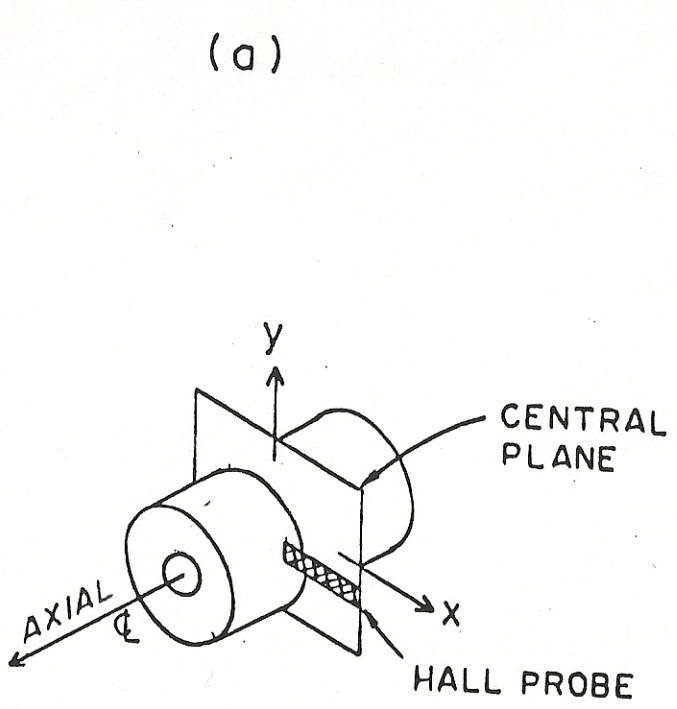

Fig.12 (a) Sketch of the Field Measurement Device.

Fig. 12 (b) Field variation along radius direction on the middle plane

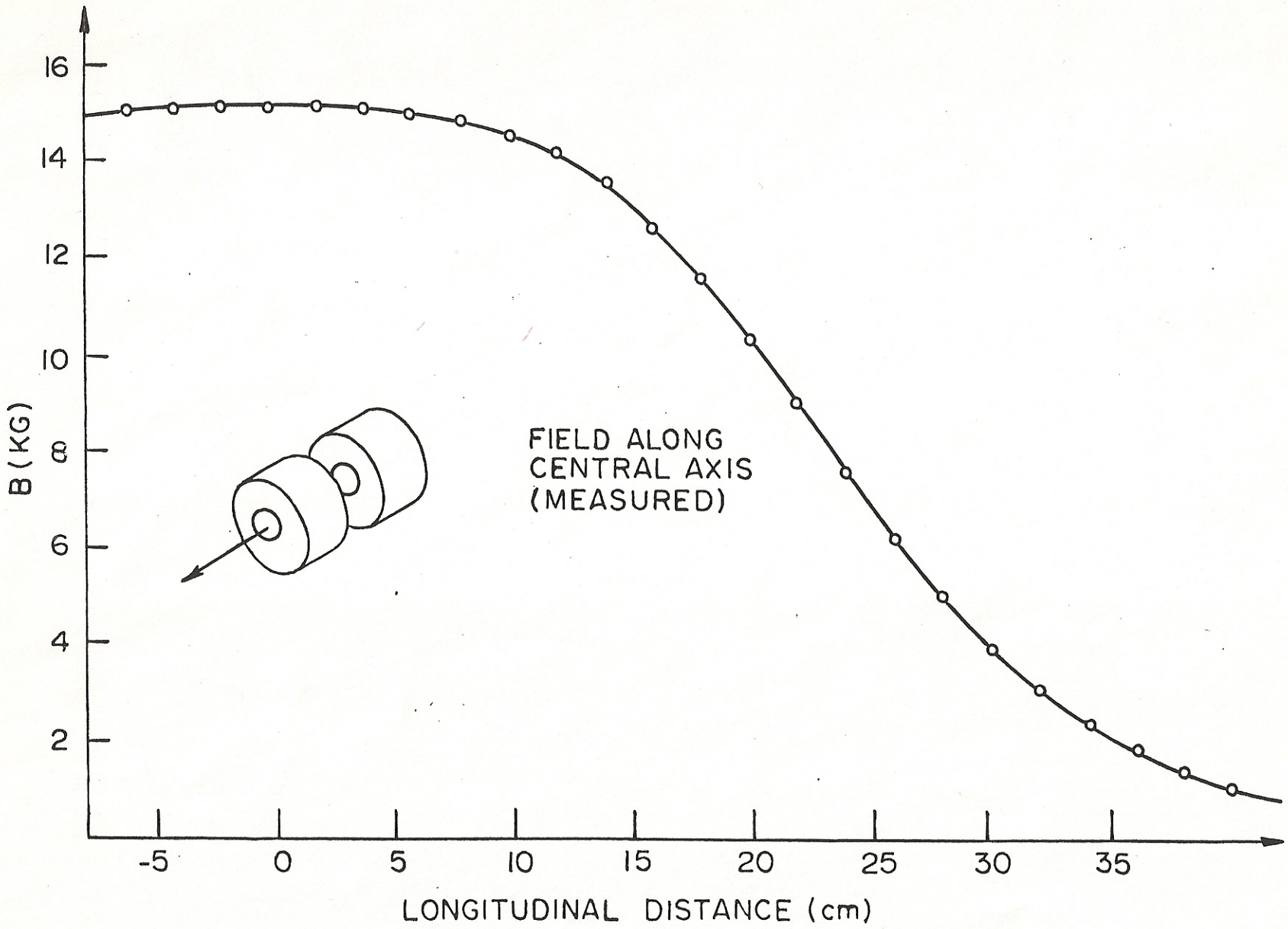

Fig. 13 Field Distribution along Longitudinal Direction

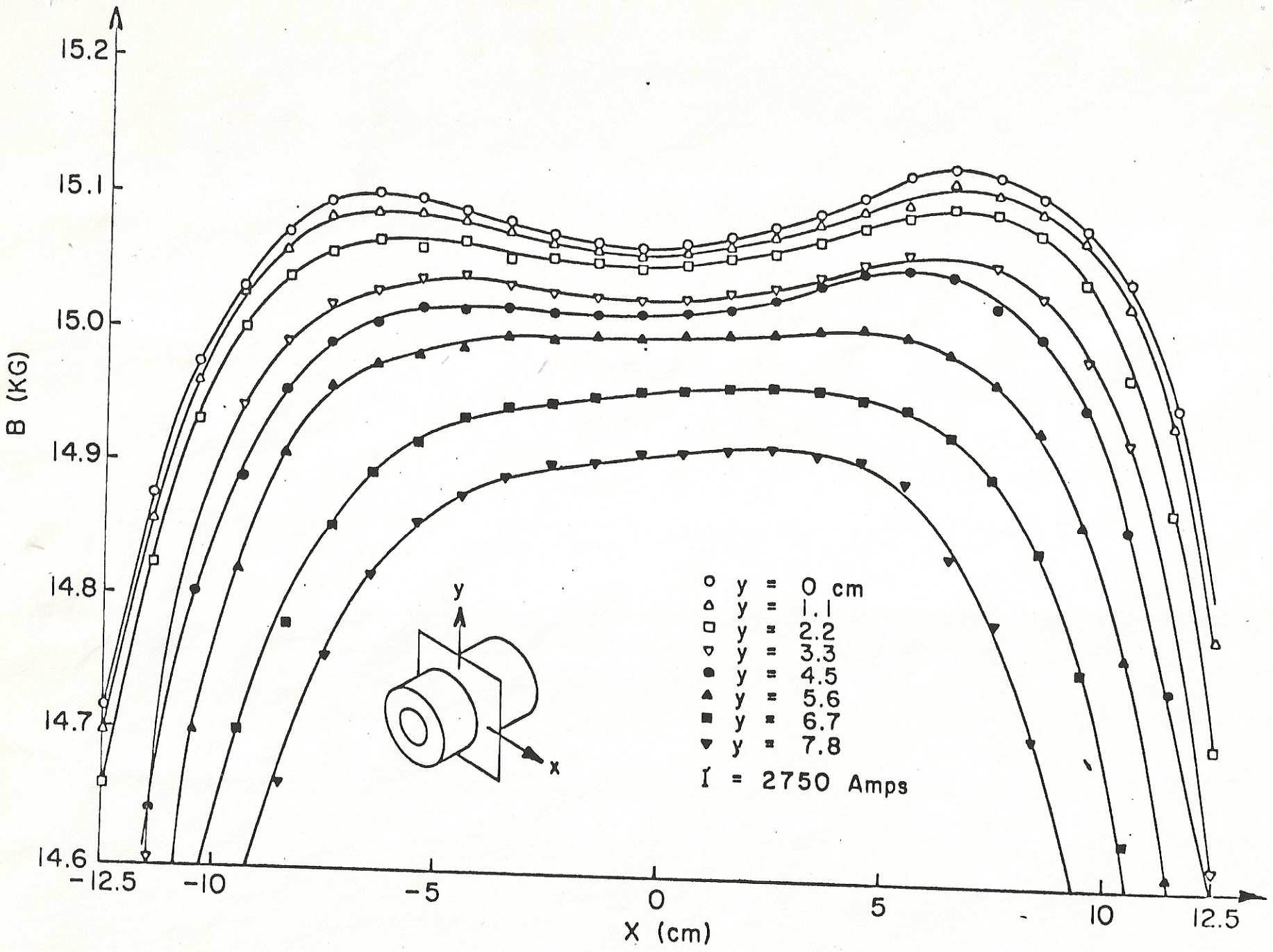

Fig. 14 Field distribution along x for different y where x, y are defined as shown.

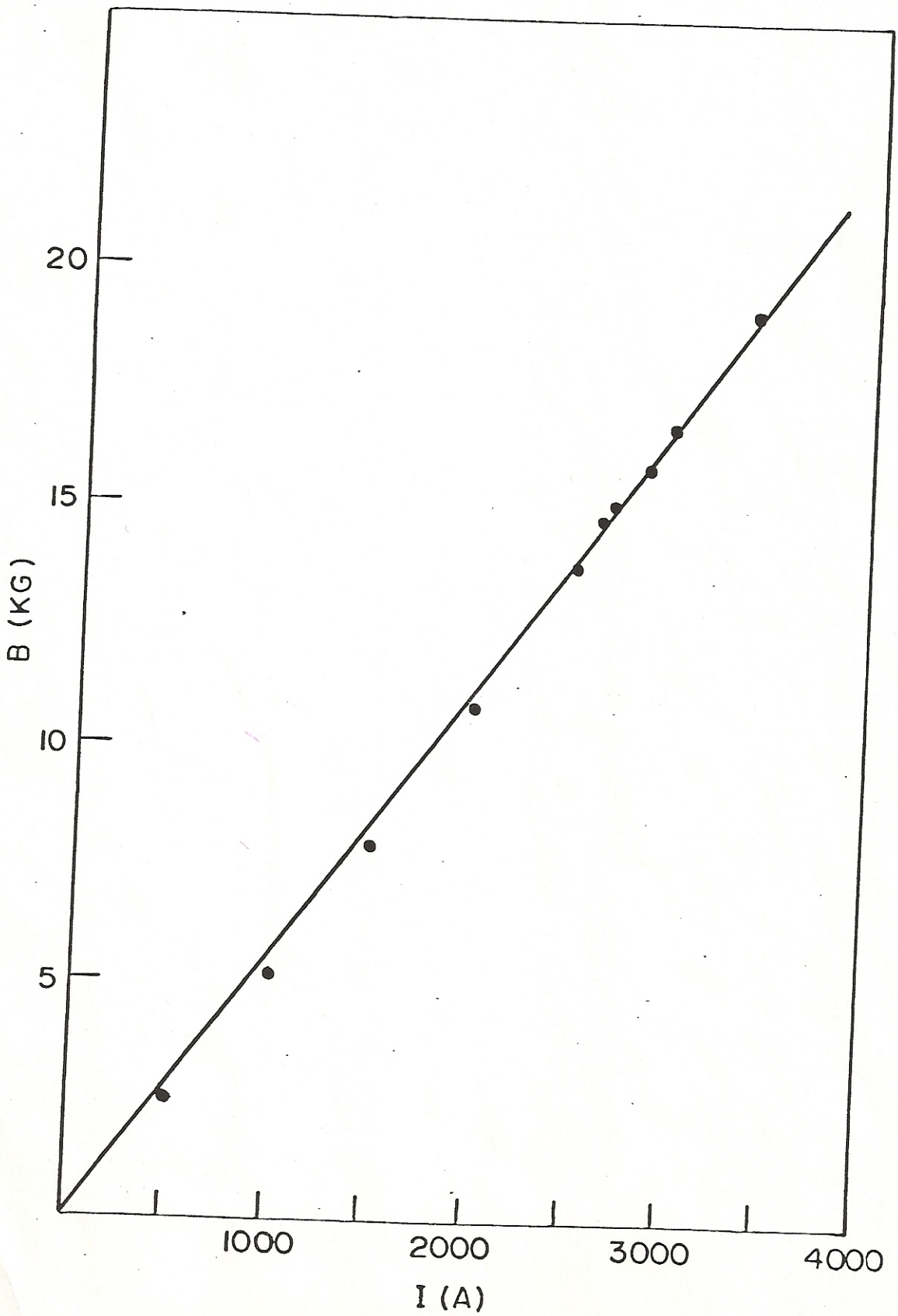

Fig. 15 Excitation curve of the magnet

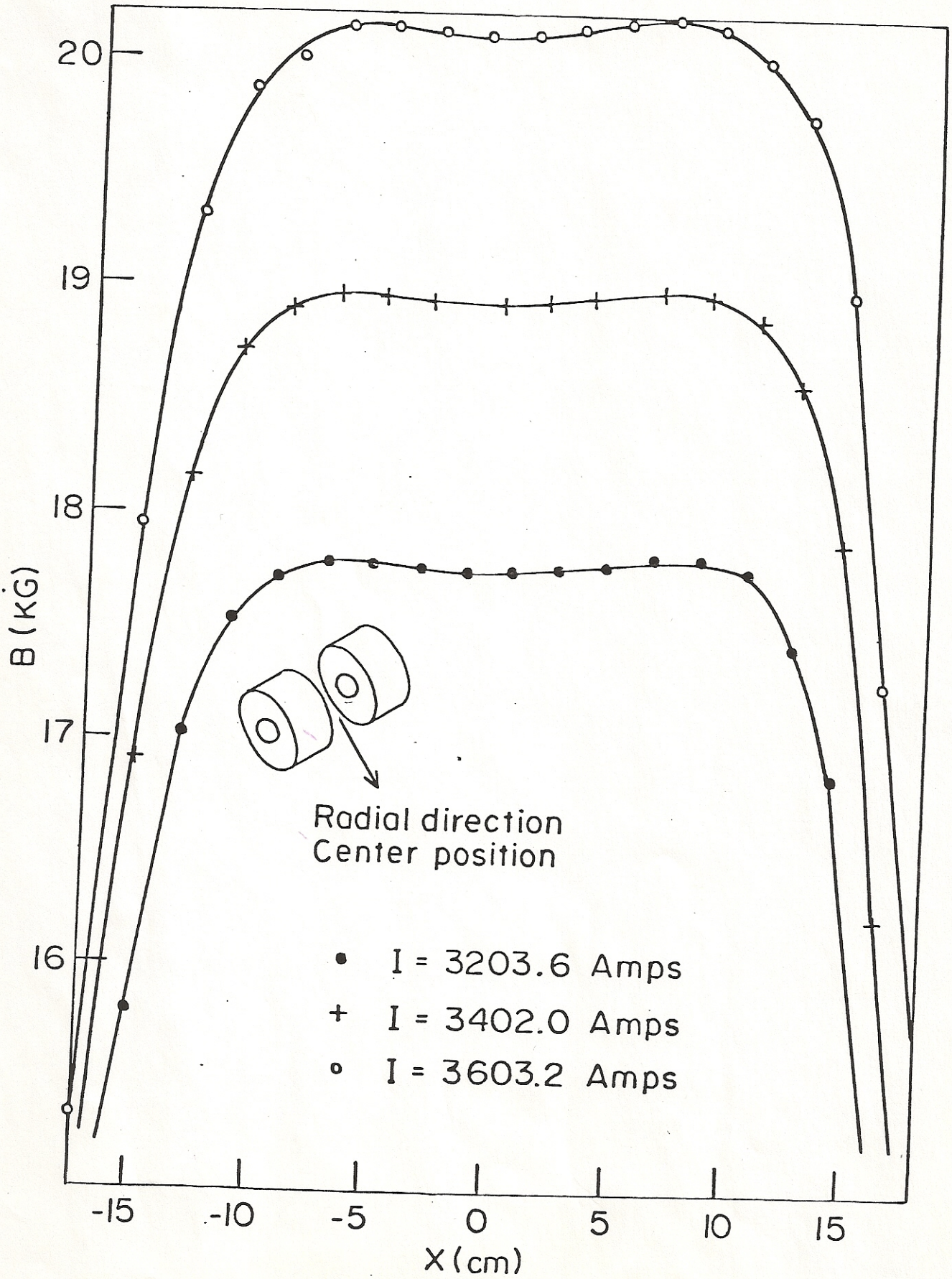

Fig. 16 Field along x at highest currents